The Journal of International Advanced Otology

J Int Adv Otol 2020; 16(2): 153-7 • DOI: 10.5152/iao.2020.7690

Original Article

New Classification of Cochlear Hypoplasia Type Malformation: Relevance in Cochlear Implantation

Roa Talal Halawani, Anandhan Dhanasingh

Ohud General Hospital, Ministry of Health, AL Medina, Kingdom of Saudi Arabia (RTH)
MED-EL GmbH, Innsbruck, Austria (AD)

ORCID iDs of the authors: R.T.H. 0000-0002-4804-4286; A.D. 0000-0003-2116-9318.

Cite this article as: Halawani RT, Dhanasingh A. New Classification of Cochlear Hypoplasia Type Malformation: Relevance in Cochlear Implantation. J Int Adv Otol 2020; 16(2): 153-7.

OBJECTIVES: This paper attempts to create a new classification type of cochlear hypoplasia (CH)-type malformation taking into consideration of vestibular section and internal auditory canal (IAC).

MATERIALS and METHODS: Preoperative computed-tomography (CT) scans of cochlear implant (CI) candidates (N=31) from various clinics across the world with CH type malformation were taken for analysis. CT dataset were loaded into 3D-slicer freeware for three-dimensional (3D) segmentation of the inner-ear by capturing complete inner-ear structures from the entire dataset. Cochlear size in terms of diameter of available cochlear basal turn and length of cochlear lumen was measured from the dataset. In addition, structural connection between IAC and cochlear portions was scrutinized, which is highly relevant to the proposed CH classification in this study.

RESULTS: CH group-I has the normal presence of IAC leading to cochlear and vestibular portions, whereas CH group-II is like CH group-I but with some degree of disruption in vestibular portion. In CH group-III, a disconnection between IAC and the cochlear portion irrespective of other features. Within all these three CH groups, the basal turn diameter varied between 3.1 mm and 9.6 mm, and the corresponding cochlear lumen length varied between 3 mm and 21 mm for the CI electrode array placement.

CONCLUSION: A new classification of CH mainly based on the IAC connecting the cochlear and vestibular portions is presented in this study. CI electrode array length could be selected based on the length of the cochlear lumen, which can be observed from the 3D image.

KEYWORDS: Three-dimensional segmentation, inner ear, cochlear hypoplasia

INTRODUCTION

Cochlear implantation (CI) is the standard of care in treating patients with sensorineural hearing loss, including inner-ear malformation types [1]. The incidence rate of CI candidates with inner-ear anatomical malformation has been reported to be around 20% in various studies by Sennaroglu et al. [2, 3]. Although the hearing performance of patients with inner-ear malformation has been reported to be highly varying with CI [4, 5], the proper electrode array placement along with the detailed analysis of the structural connection between cochlea and the internal auditory canal (IAC) is essential.

Irrespective of inner-ear malformation types, it is essential to look for the availability of the cochlear lumen for the CI electrode array placement and the presence of the cochlear nerve (CN) for carrying the electrical stimulus from the electrode to the brain. The presence and absence of the vestibular portion on a patient's hearing performance with CI is still not understood. The current inner-ear malformation types including incomplete partition type I, II, and III and cochlear hypoplasia (CH) are mainly based on internal structural architecture of the cochlear portion alone [6]. The common cavity is the only malformation type that includes the vestibular portion [7]. CN aplasia simply focuses on the absence of CN irrespective of other inner-ear structures. Although the previous cochlear malformation type classifications were mainly based on size and number of turns of the cochlear portion, the CN and vestibular portion have not been taken into serious consideration. The incidence rate of CH with an inner-ear malformation is reported to be 15%-23% [4, 8], showing the predominance of this malformation type.

This study was presented by the second author at the 14th European Symposium on Pediatric Cochlear Implantation, Bucharest, Romania.

Corresponding Address: Roa Talal Halawani E-mail: Roa_halawani@yahoo.com

Submitted: 09.04.2019 • **Revision Received:** 01.13.2020 • **Accepted:** 02.10.2020
Available online at www.advancedotology.org

In general, it could be a challenging task to mentally compile series of CT image slices for corresponding anatomical structures in 3D. In order to simplify the visualization of inner-ear structures, we propose the method of 3D segmentation that could be applied to the entire inner-ear structures. Also, we attempt to create a new classification of CH-type malformations by taking the IAC and the vestibular portion into consideration. This could prove to be a valuable tool for Ear Nose Throat (ENT) surgeons to visualize the complete inner-ear and get an understanding on the malformation type before opening the mastoid for placement of the CI electrode.

MATERIALS AND METHODS

Preoperative computed-tomography (CT) scans of anonymized cochlear implant (CI) candidates (N=31) from various clinics across the world with CH type malformation identified were taken for analysis. The CT data set collection took place between the year 2011 and 2018. CT dataset was loaded into a 3D slicer freeware (3D Slicer, version 4.8.0, Massachusetts, USA) for the 3D segmentation of complete inner-ear structures. Steps involved in the 3D segmentation of inner ear is described elsewhere [9, 10]. In brief, the image datasets were loaded into the 3D slicer freeware. Subsequently, the complete inner-ear structures were captured, including the IAC in all image slices. An axial plane is better for segmentation of these structures by setting a tight grayscale threshold to avoid capturing undesired structures (Figure 1). Figure 1 elaborates the segmentation process. Segmentation of the complete inner ear including the IAC from clinical imaging dataset takes approximately 10 minutes. The size of the cochlear portion was measured by the "A" value as proposed by Escude et al. [11], and the length of cochlear lumen for the CI electrode array placement is determined by going along the outer wall to the extent to which the cochlea is developed, as shown in Figure 1.

Statistical Analysis

Microsoft Excel (Microsoft Corp., Redmond, Washington, USA) was used in finding the mathematical relations between various parameters of the inner ear.

RESULTS

From the 31 preoperative high-resolution CT (HRCT)–image dataset of the human temporal bones, we were able to group five datasets that had a near-normal vestibular portion and the IAC under CH group-I. In CH group-II, 15 datasets with partial disruption in the vestibular portion but with near-normal IAC were identified, and the remaining 11 datasets that had either partial or complete disruption of the vestibular portion and the IAC were grouped under CH group-III.

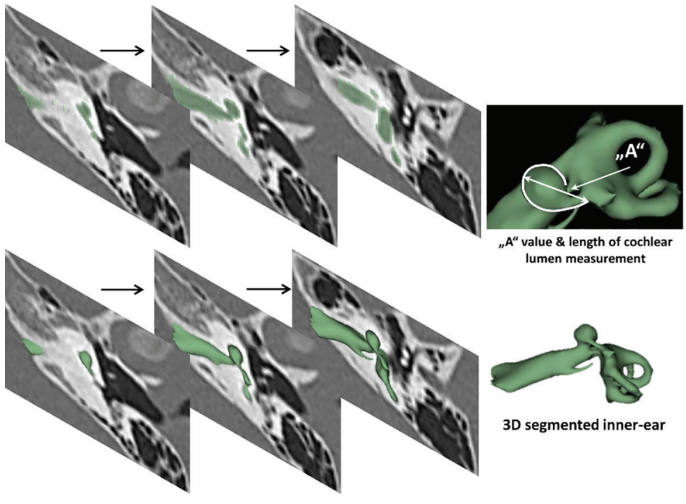

Figure 1. The 3D segmentation of the inner ear by capturing the inner-ear structures from all the images slices. The cochlear size was measured by following the outer wall of the cochlea, shown by the curved white line.

CH group-I

Cochlear portions of all sizes were classified under this group, with the complete presence of the vestibular portion and a structural connection between the cochlea and IAC (Table 1). Samples a-c showed good presence of the cochlear portion that goes beyond the basal turn. Samples d and e showed a small bud–like cochlear. The size of the cochlea, as measured by the "A" value, varied between 3 mm and 8 mm, which correspondingly related linearly to the length of the cochlear lumen measured, which varied between 12 mm and 21 mm (Figure 2).

CH group-II

CH group-II was characterized by partial to full disruption of the vestibular portion (Table 2). Samples a-f showed the hypoplastic vestibular portion with three distinct semicircular canals. Samples g-m is

Table 1. CH group I

S.No	Coronal	Axial	Length of Cochlear lumen (mm)	"A" value (mm)
a			21	7
b			20	6.5
c		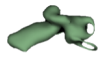	17	8.0
d			12	3.2
e			12	3.1

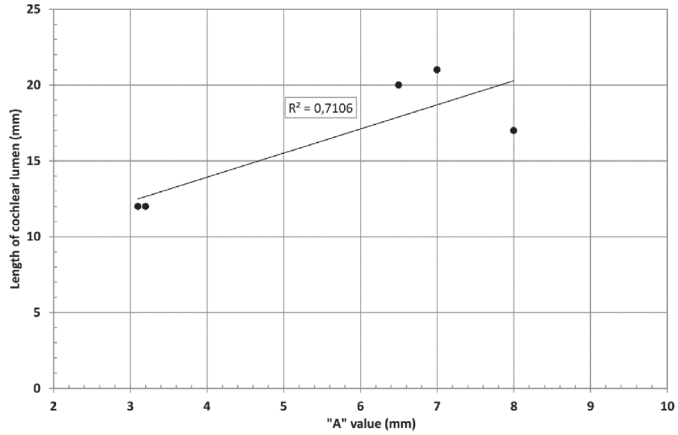

Figure 2. "A" value vs length of cochlear lumen in CH group–I showed a linear positive relation.

Table 2a. CH type II

S.No	Coronal	Axial	Length of Cochlear lumen (mm)	"A" value (mm)
a			15	6.9
b			16	6.8
c			16	7.4
d			16	7.3
e			19	6.8
f			10	8.1
g			13	8.2
h			12	7.0
i			17	8.4
j			16	9.6
k			20	8.5
l			12	5.6
m			3.0	-
n			20	9.0
o			16	7.8

Table 2b. CH type III (Continued)

S.No	Coronal	Axial	Length of Cochlear lumen (mm)	"A" value (mm)
a			19	8.1
b			6	-
c			12	6.6
d		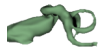	13	6.5
e			19	7.3
f			8	4.9
g			7	4.8
h			7,8	7
i			19	7.2
j			19	8.4
k			6	-

Figure 3. "A" value vs length of cochlear lumen in CH group–II with a linear positive relation.

characterized by a distorted vestibular portion with the presence of one or two semicircular canals. Clearly, samples n and o are lacking all the semicircular canals. In all these samples, the size and shape of the cochlear portion are highly variable, with the measured "A" value ranging from 5.6 mm and 9.6 mm. The corresponding length of the cochlear lumen varied linearly between 10 mm and 20 mm (Figure 3).

CH group-III

Although all the samples given under CH group-III (Table 3) have the IAC in place, they lack the structural connection to the cochlear portion. Samples a and b have a clear structural disconnection between IAC and the cochlear portion, whereas samples c-k showed IAC structurally connecting to the vestibule. Samples j and k lack the vestibular portion completely in addition to the structural disconnection between the IAC and the cochlear portion. The cochlear size,

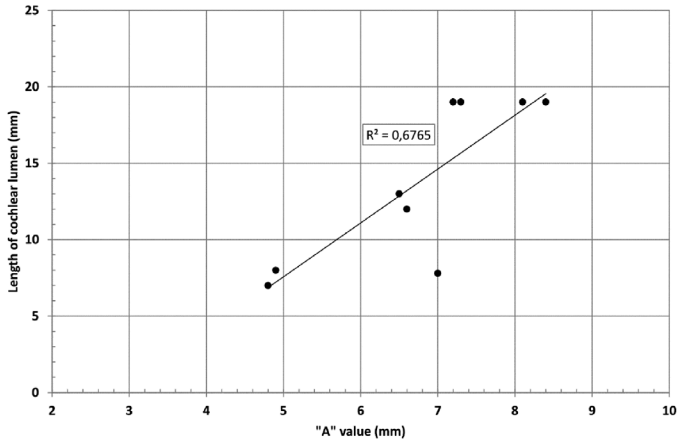

Figure 4. "A" value vs length of cochlear lumen in CH group–III showing a linear positive relation.

as measured by the "A" value, ranged from 4.8 mm to 8.4 mm and was linearly correlated to the length of cochlear lumen, which varied between 7 mm and 19 mm (Figure 4).

DISCUSSION

Knowing the availability of the cochlear lumen is of at most importance for the CI electrode placement. The other structures, especially the IAC connecting the cochlea, should also be analyzed carefully before the CI surgery. For CH group-I, with samples a-e given in Table 1, the cochlear size and number of turns vary almost from a small bud-like appearance (d, e) to one full turn of the cochlear lumen (a-c). The choice of CI electrode array for these cochlear sizes and shapes could easily vary from auditory brainstem implant (d and e) to a 15-20 mm long CI electrode array (a-c).

The samples in CH group-II, given in Table 2, were placed in an order starting with those that had the vestibular portion with three distinct semicircular canals (a-f) followed by the presence of either one or two semicircular canals (g-m) and the complete absence of vestibular portion (n and o). CI electrode array length should be chosen based on the cochlear lumen availability. In that respect, an electrode array length of 15-20 mm might be the suitable choice for samples given under this type, except sample m, taken for analysis in this study.

Samples a-k given in Table 3, representing CH group-III, are considered severe malformation because the IAC either makes no structural connection with the cochlear portion (as shown in samples a and b) or is structurally connected only to the vestibular portion (as shown in samples c-k). Implanting a CI in the CH group-III may not be the best choice as lack of structural connection from the cochlea to the IAC would prevent the passage of electrical stimulation from the cochlea to the other levels in the auditory pathway. Birman et al. [12] reported that the hearing performance of CI patients improved after CI treatment even with CN aplasia detected. This is further supported by Warren et al. [13], but with the suggestion of evaluating the patient with electrically evoked auditory brainstem response. Papsin et al. [14] reported that patients with CN aplasia are poor performers compared with patients with other inner-ear malformations, which must be considered while counseling the patients. Last author of this study received an anonymized

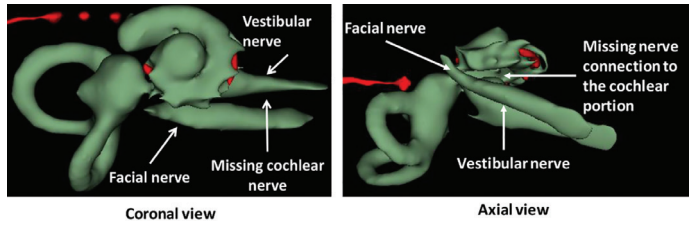

Figure 5. Postoperative image in both coronal and axial views clearly showing the absence of the CN.

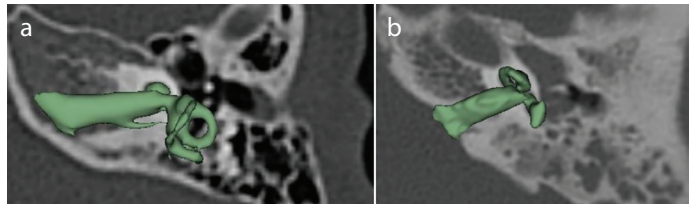

Figure 6. a, b. a) CH with normal presence of vestibular portion. b) CH with absence of the three semicircular canals of the vestibular portion.

postoperative image dataset from a case in which the patient was implanted with CI and did not receive any benefit from the device. 3D segmentation of the inner ear (Figure 5) with the electrode inside clearly revealed the absence of the CN, but with the presence of facial and vestibular nerves.

The importance of the presence and absence of the vestibular portion in relation to surgical difficulty or ease is interesting from the surgeon's perspective. Figures 6 compare two situations—with and without the semicircular canals of vestibular portion.

3D visualization of the complete inner-ear along with the two-dimensional radiographic image certainly adds valuable information both in understanding the morphology of all the inner-ear structures and in surgical pre-planning.

CONCLUSION

The 3D segmentation of the inner ear could be performed as a standard procedure during preoperative image analysis, which adds valuable information both in understanding outer morphology of inner ear and in surgical pre-planning. Irrespective of cochlear size and shape, clear structural connection between IAC and the cochlear portion needs to be analyzed and CI electrode array length then can be selected simply based on cochlear size and shape, which can be measured from the 3D image.

Ethics Committee Approval: N/A.

Informed Consent: N/A.

Peer-review: Externally peer-reviewed.

Author Contributions: Concept – R.H., A.D.; Design – R.H., A.D.; Supervision – A.D.; Resource – R.H.; Materials – R.H.; Data Collection and/or Processing – R.H.; Analysis and/or Interpretation – A.D., R.H.; Literature Search – A.D., R.H.; Writing – A.D., R.H.; Critical Reviews – A.D.

Acknowledgements: Authors thank all those clinics across the world for sharing the anonymized CT images of temporal bones of patients with inner-ear malformation for educational purposes. Ms. Dijana Mitrovic from MED-EL is kindly acknowledged for her assistance in 3D slicer software.

Conflict of Interest: Anandhan E. Dhanasingh is employed by MED-EL GmbH, Austria as the Head of Translational Science Communication which is purely scientific roles with no marketing activities.

Financial Disclosure: The authors declared that this study has received no financial support.

REFERENCES

1. Farhood Z, Nguyen SA, Miller SC, Holcomb MA, Meyer TA, Rizk HG. Cochlear implantation in inner ear malformations: Systemic review of speech perception outcomes and intraoperative findings. Otolaryngol Head Neck Surg 2017; 156: 783-93. [Crossref]
2. Sennaroglu L, Baijin MD. Classification and current management of inner ear malformations. Balkan Med J 2017; 34: 397-411. [Crossref]
3. Sennaroglu L. Cochlear implantation in inner ear malformations- a review article. Cochlear Implants Int 2010; 11: 4-41. [Crossref]
4. Cinar BC, Batuk MO, Tahir E, Sennaroglu G, Sennaroglu L. Audiologic and radiologic findings in cochlear hypoplasia. Auris Nasus Larynk 2017; 44: 655-63. [Crossref]
5. Qi S, Kong Y, Xu T, Dong R, Lv J, Wang X, et al. Speech development in young children with mondini dysplasia who had undergone cochlear implantation. Int J Pediatr Otorhinolaryngol 2019; 116: 118-24. [Crossref]
6. Sennaroglu L. Histopathology of inner ear malformations: Do we have enough evidence to explain pathophysiology? Cochlear Implants Int 2016; 17: 3-20. [Crossref]
7. Huang BY, Zdanski C, Castillo M. Pediatric sensorineural hearing loss, part 1: practical aspects for neuroradiologists. AJNR Am J Neuroradiol 2012; 33: 211-7. [Crossref]
8. Joshi VM, Navlekar SK, Kishore GR, Reddy KJ, Kumar ECV. CT and MR imaging of the inner ear and brain in children with congenital sensorineural hearing loss. Radiographics 2012; 32: 43-8. [Crossref]
9. Dhanasingh A. Variation in the size and shape of human cochlear malformation types. Anat Rec (Hoboken) 2019; 302: 1792-9. [Crossref]
10. Dhanasingh A, Dietz A, Jolly C, Roland P. Human inner-ear malformation types captured in 3D. J Int Adv Otol 2019; 15: 77-82. [Crossref]
11. Escude B, James C, Deguine O, Cochard N, Eter E, Fraysse B. The size of the cochlea and predictions of insertion depth angles for cochlear implant electrodes. Audiol Neurootol 2006; 11 Suppl 1: 27-33. [Crossref]
12. Birman CS, Powel HR, Gibson WP, Elliot EJ. Cochlear implant outcomes in cochlear nerve aplasia and hypoplasia. Otol Neurotol 2016; 37: 438-45. [Crossref]
13. Warren FM, Wiggins RH, Pitt C, Harnsberger HR, Shelton C. Apparent cochlear nerve aplasia: to implant or not to implant? Otol Neurotol 2010; 31: 1088-94. [Crossref]
14. Papsin BC. Cochlear implantation in children with anomalous cochleovestibular anatomy. Laryngoscope 2005; 115: 1-26. [Crossref]